DOI: 10.1002/adma.200600155

Pathways for Resonant Energy Transfer in Oligo(phenylenevinylene)–Fullerene Dyads: An Atomistic Model**

By *Terttu I. Hukka*, *Teemu Toivonen*, *Emmanuelle Hennebicq*, *Jean-Luc Brédas*, *René A. J. Janssen*, and *David Beljonne**

In the quest for renewable energy, an increasing amount of attention is devoted to the use of organic conjugated materials as active components in photovoltaic devices. Because the primary photoexcitations in conjugated molecules and polymers are strongly bound electron–hole pairs (excitons), efficient charge generation only takes place at the heterojunction between a low-ionization-potential (electron-donor) material and a high-electron-affinity (electron-acceptor) material in multicomponent architectures. This provides the energy mismatch between the frontier molecular orbitals required to overcome the exciton binding energy, which is on the order of 0.4 eV in conjugated polymers.[1–4] The highest quantum yields for charge generation in organic cells to date have been reported for polymer–fullerene blends.[5,6] C_{60} is an efficient electron acceptor but features reduced absorption cross section in the visible spectral region due to symmetry-forbidden optical transitions (note that these symmetry constraints are slightly relaxed in the soluble C_{60} derivatives such as [6,6]-phenyl C_{61}-butyric acid methyl ester (PCBM)[7]). Thus, in the simplest scenario, photoinduced charge generation in polymer–fullerene cells involves the formation of a local excited state on the conjugated polymer, which acts both as electron donor and sensitizer, followed by electron transfer to C_{60}.

A different picture was proposed on the basis of time-resolved transient[8] and photoluminescence quenching[9] experiments performed in solutions of model dyad and triad compounds including oligo(phenylenevinylene) (OPV_n) as donor and *N*-methylfulleropyrrolidine (MPC_{60}) as acceptor.[8–10] The solution data suggest a two-step mechanism with resonant energy transfer (RET) from the photoexcited conjugated chain to the covalently linked fullerene derivative *prior* to hole migration from MPC_{60} to the OPV_n moiety. In films, the direct photoinduced electron-transfer reaction is much faster than in solution as a result of more favorable donor–acceptor interactions, and the dynamics of direct electron transfer versus RET can no longer be distinguished using femtosecond pump–probe spectroscopy.[11,12] Thus, the two competitive channels (electron transfer versus RET followed by hole transfer) likely contribute to charge generation in solid-state photovoltaic devices. We note that energy transfer has also been demonstrated to compete with charge generation in other C_{60}-based molecular dyads.[13,14]

Two questions arise at this stage. First, can one take advantage of RET to design more efficient polymer-based photovoltaic cells? A threefold increase in photocurrent has been recently reported by McGehee and co-workers on inserting a thin layer of a low-bandgap polymer at the interface between a polythiophene derivative (donor) and TiO_2 (acceptor).[15] The enhanced charge generation quantum yield was ascribed to RET to the low-bandgap material and the resulting improved harvesting of electronic excitations at the donor–acceptor heterojunction. Such a directional excitation-migration process indeed allows for controlled energy funneling to specific interfacial sites, which is often not the case for random diffusion in disordered conjugated polymers (where excitations can get trapped at low-energy sites associated with defects or aggregates[16–19]). On the other hand, the design strategies for donor and acceptor chemical structures in fullerene-based polymer solar cells have so far largely been based on the energetics and dynamics of electron-transfer processes. These might have to be reconsidered when hole transfer plays

[*] Dr. D. Beljonne, Dr. E. Hennebicq, Prof. J.-L. Brédas
Laboratory for Chemistry of Novel Materials
University of Mons-Hainaut
Place du Parc 20, 7000 Mons (Belgium)
E-mail: David@averell.umh.ac.be
Dr. D. Beljonne, Dr. T. I. Hukka, Prof. J.-L. Brédas
School of Chemistry and Biochemistry and
Center for Organic Photonics and Electronics
Georgia Institute of Technology
Atlanta, GA 30331-0400 (USA)
Dr. T. I. Hukka, T. Toivonen
Institute of Materials Chemistry, Tampere University of Technology
P.O. Box 541, 33101 Tampere (Finland)
Prof. R. A. J. Janssen
Laboratory of Macromolecular and Organic Chemistry
Eindhoven University of Technology
P.O. Box 513, 5600 MB Eindhoven (The Netherlands)

[**] The work at Georgia Tech is partly supported by the Office of Naval Research and by the National Science Foundation (through STC Award DMR-0120967 and CRIF Award CHE-0443564). The work at Tampere University of Technology is supported by the Academy of Finland. T. I. Hukka also thanks Georgia Institute of Technology for a research fellowship. The work in Mons is partly supported by the Belgian Federal Government "Interuniversity Attraction Pole in Supramolecular Chemistry and Catalysis, PAI 5/3", the European Integrated Project NAIMO (NMP4-CT-2004-500355), and the Belgian National Fund for Scientific Research (FNRS/FRFC). E. H. and D. B. are FNRS Postdoctoral Researcher and Research Associate, respectively.

ADVANCED MATERIALS

an important role, as, e.g., the driving force and electronic coupling entering a Marcus-like treatment of photoinduced charge-transfer rates will likely be different for hole transfer versus electron transfer.[20]

The second question that is addressed in the present work is: How can one reconcile the fast RET measured in OPV_n–MPC_{60} dyads with the low absorption intensity of the fullerene derivative in the visible spectral region? From a simple Förster model, fast RET indeed requires overlap between the donor emission and acceptor absorption spectra, combined with strong dipole–dipole coupling between the chromophores. However, because of symmetry selection rules, the local excitations over the MPC_{60} unit that are in close resonance with the lowest (emitting) excited state of the OPV_n segment display small transition dipole moments, a feature that is seemingly at odds with the measured fast energy-transfer rates. As a matter of fact, it was shown that the Förster model can reproduce the RET rate measured in an OPV_4–MPC_{60} toluene solution only by making the unreasonable assumption that the effective distance between the interacting point dipoles is less than half the actual donor–acceptor center-to-center separation.[9]

We recall that the point-dipole model "averages away" the shapes of the donor and acceptor wavefunctions and can only be applied when the size of the interacting molecules is small with respect to the intermolecular separation.[21] To account for the detailed chemical structure and topology of the interacting chromophores, we have worked on the basis of an "improved" Förster formalism, wherein the total electronic coupling is expressed as a sum over pairwise interactions between atomic-transition charges.[22–26] In addition, because of its 3D structure, C_{60} displays a high density of low-lying excited states and, hence, many pathways can potentially contribute to the overall energy-transfer rate. We show below that, when including these contributions within an improved Förster approach, rates in reasonable agreement with experiment are obtained.

The simulated OPV_n photoluminescence spectra (for $n = 2$–4) and MPC_{60} absorption spectra are shown in Figure 1. As expected, increasing the number of repeat units in the alkoxy-substituted OPV donor molecule results in a bathochromic shift of the INDO/SCI-computed (INDO: intermediate neglect of differential overlap; SCI: single-configuration interaction) $S_1 \rightarrow S_0$ optical transition from ca. 3.0 eV in OPV_2 down to ca. 2.5 eV in OPV_4; these values are in excellent agreement with experiment.[8,9] The overall shape of the absorption spectrum of the MPC_{60} solution is also well accounted for by the INDO/SCI calculations: in the high-energy spectral range, it displays a main peak at ca. 3.8 eV (versus a computed value of ca. 3.95 eV) together with a broad tail spanning the whole visible range. On the low-energy side of the spectrum, one can identify two very weak bands at ca. 2.2 eV (lowest excited state) and ca. 2.6 eV followed by additional and slightly more intense features at ca. 2.9 eV (peak), ca. 3.2 eV (shoulder), and ca. 3.5 eV (shoulder); the 2.9 eV feature likely corresponds to the first somewhat well-defined peak emerging from the broad absorption background and measured at ca. 3 eV in MPC_{60} toluene solutions. We will come back to the assignment of these electronic transitions below.

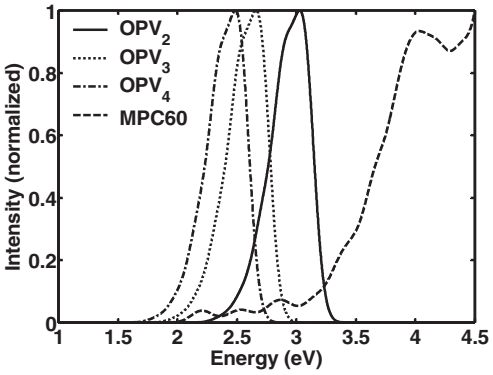

Figure 1. Emission spectra of OPV_n, $n = 2$–4, and absorption spectrum of MPC_{60}, as simulated on the basis of an INDO/SCI (INDO: intermediate neglect of differential overlap; SCI: singles-configuration interaction) description of the singlet excited states. See text for details.

Table 1 compares the measured[8] and calculated (see Experimental section) energy-transfer rates in the three molecules. Taking into account the crudeness of the model applied here to describe the MPC_{60} absorption lineshape, the theoretical rates are in good agreement with the corresponding experimental values (although the calculations yield a stronger chain-length dependence than what was measured). The donor–acceptor exciton migration (hopping) times are found in all cases to be in the picosecond or sub-picosecond range. The decrease in transfer rate with increasing oligomer length can be ascribed to weaker electronic interactions as the center-to-center separation between the OPV_n and MPC_{60} molecules increases.

Table 1. Calculated and experimental energy-transfer rate constants (k_{RET}) in OPV_n–MPC_{60} dyads and OPV_n–C_{60} "thought" complexes. The numbers in parentheses correspond to the Förster rates and the point-dipole approximation.

Compound	k_{RET} [$\times 10^{12}$ s^{-1}]	
	Calculated	Experimental [a]
OPV_2–MPC_{60}	6.6 (1.1)	2.9
OPV_3–MPC_{60}	2.3 (0.3)	2.1
OPV_4–MPC_{60}	0.5 (0.1)	1.1
OPV_2–C_{60}	1.9 (0.9)	–
OPV_3–C_{60}	2.9 (0.1×10^{-3})	–
OPV_4–C_{60}	1.2 (0.1×10^{-6})	–

[a] Experimental values are from the compounds in toluene, obtained from the literature [8].

For the sake of comparison, we also list in Table 1 the Förster rates obtained within the point-dipole approximation (here, the electronic couplings are computed by considering two point dipoles located at the centers of the donor and acceptor fragments, accounting for their relative orientations via

the usual geometric factor[27]). Clearly, the point-dipole model severely underestimates (by almost one order of magnitude) the energy-transfer rates with respect to the multicentric transition-density approach, a feature that has been largely discussed previously in the case of "head-to-head" configurations similar to those found here for the OPV_n–MPC_{60} dyads.[25] The shortcoming of the point-dipole model is related to the fact that the actual electronic couplings in such configurations are dominated by contributions to the excited-state wavefunctions arising from the donor and acceptor molecular edges that are in close contact within the dyad architecture (since these lead to the shortest donor–acceptor interatomic distances). To account for these effects, it is essential to go beyond the point-dipole approximation, as done here via the use of atom-based transition charges (see Experimental).

Table 2 shows the contributions ($k_{i_d-j_a}$) to the total exciton hopping rates from the main pathways associated to acceptor states, j_a (i_d is the lowest donor (OPV_n) excited state), together with the corresponding electronic couplings ($V_{i_d-j_a}$) and spectral-overlap factors ($J_{i_d-j_a}$). For the three dyads, we have identified a few (typically five) acceptor excited states that simultaneously lead to significant $V_{i_d-j_a}$ and $J_{i_d-j_a}$ values. These belong to the 2.6, 2.9, and 3.2 eV absorption features discussed above, with relative contributions depending on the match with the donor excited-state energy (i.e., the largest contributions arise from the 2.9 and 3.2 eV bands in the shortest ($n=2$ and $n=3$) OPVs and from the 2.6 eV band for the longest ($n=4$) donor segment).

Table 2. Contributions $k_{i_d-j_a}$ to the total energy hopping rates k_{RET} from the dominant pathways associated to MPC_{60} acceptor states j_a. The excitation energies, electronic couplings, and spectral-overlap factors are also indicated for each channel.

Dyad	MPC60 excited state, j_a	Transition energy [eV]	$k_{i_d-j_a}$ [$\times 10^{12} s^{-1}$]	$V_{i_d-j_a}$ [cm^{-1}]	$J_{i_d-j_a}$ [$\times 10^{-3}$ cm]
OPV_2–MPC_{60}	S_{12}	2.72	0.4	52	0.13
	S_{15}	2.81	2.5	104	0.19
	S_{19}	3.05	0.6	45	0.24
	S_{20}	3.06	0.6	47	0.24
	S_{25}	3.16	0.8	69	0.14
OPV_3–MPC_{60}	S_6	2.49	0.1	21	0.22
	S_8	2.58	0.3	30	0.26
	S_9	2.63	0.6	43	0.26
	S_{12}	2.72	0.3	37	0.21
	S_{15}	2.81	0.8	75	0.12
OPV_4–MPC_{60}	S_6	2.49	0.07	15	0.26
	S_8	2.58	0.12	24	0.18
	S_9	2.63	0.15	31	0.13
	S_{12}	2.72	0.03	24	0.04
	S_{15}	2.81	0.03	50	0.009

An in-depth analysis of the nature of the lowest singlet electronic excitations in C_{60} and C_{70} has been reported by Orlandi and Negri on the basis of semiempirical quantum-chemical calculations.[28] The overall picture emerging from this theoretical study can be summarized in the following way. While C_{60} features a first dipole-allowed electronic excitation in the UV spectral range (calculated well above—by about 1 eV—the transitions to the lowest dipole-forbidden excited states), the reduced symmetry in C_{70} leads to a more complicated pattern, namely, with the presence of multiple well-defined allowed transitions in the visible or near-UV spectral range.

Similar symmetry-lowering effects are anticipated for the MPC_{60} derivative. Comparison between the INDO/SCI simulated C_{60} and MPC_{60} absorption spectra (Fig. 2) partly supports this view, yet the reshuffling in excited-state energies and oscillator strengths induced by deforming the fullerene cage is relatively limited in MPC_{60}: upon switching from C_{60} to MPC_{60}, the overall shape of the absorption spectrum is indeed maintained, the predominant absorption features are broadened but hardly shifted, and the lowest singlet excited states acquire a very limited cross section (all excited states below 3.5 eV display transition dipole moments smaller than or on the order of 1 D). Similar relatively minor changes are observed experimentally from room-temperature optical-absorption measurements in C_{60}[29] and MPC_{60}[8,9] solutions. In particular, both molecules show a small bump at ca. 3.0 eV superimposed on a continuous background absorption, and a strong band that peaks at ca. 3.8 eV.

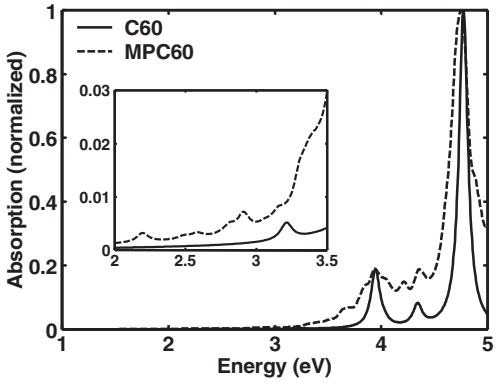

Figure 2. Comparison between the INDO/SCI simulated C_{60} and MPC_{60} absorption spectra. A magnified view of the 2.0–3.5 eV spectral range is shown in the inset.

As the perturbation induced by grafting pyrrolidine units on the C_{60} core turns out to be rather weak, the nature of the singlet electronic excitations in the soluble MPC_{60} derivative can be traced back, to a first approximation, to those in the unsubstituted fullerene compound. In particular, the excited states contributing to the weak 2.6 eV band (and features below) in the simulated spectrum of MPC_{60} correspond to symmetry-forbidden excited states in C_{60}; similarly, the first symmetry-allowed excitations in C_{60} (T_{1u} symmetry under the icosahedral I_h symmetry group) lead to the more intense 2.9 and 3.2 eV features in the substituted derivative. This is supported by the transition-density distributions displayed in

ADVANCED MATERIALS

Figure 3 for the excited states that contribute the most to the energy-transfer rates: The singlet excited state, S_9, located at 2.63 eV above the ground state, involves local rearrangements of the electronic density, with alternating positive and negative contributions that almost exactly cancel each other (the resulting transition moment is ca. 0.1 D). In contrast, electronic excitations to S_{15} at 2.81 eV and S_{25} at 3.16 eV trigger somewhat longer-range reorganization of the charge density and yield slightly larger transition dipoles (ca. 0.6 D for both states).

It is interesting to note that the electronic transitions to S_{15} and S_{25} feature orthogonal polarizations, with the former transition dipole oriented mostly along the fullerene radius passing by the pyrrolidine unit (i.e., almost perpendicular to the OPV_n–MPC_{60} connecting bond) and the latter in the plane perpendicular to this radius. Under I_h symmetry, the x, y, and z components of the dipole operator transform as T_{1u}, so that optical transitions to T_{1u}-symmetry excited states should, in principle, be unpolarized in molecules with perfect spherical symmetry. The presence of electronic excitations with T_{1u} parentage yet different polarizations in MPC_{60}, therefore, arises from the reduced symmetry in the fullerene derivative. Most importantly, the analysis in Table 2 shows that acceptor excited states leading to optical transitions that are either almost forbidden (S_9) or polarized perpendicularly to the donor emission dipole (S_{15}) act as efficient lending states for energy hopping to MPC_{60}. This result is once again in marked contrast with the expectations based on traditional Förster theory and the point-dipole approximation.

The lowest electronic excitations, which are strictly dipole-forbidden in C_{60} because of symmetry constraints (at least within the Franck–Condon approximation), acquire a very limited absorption cross section in the MPC_{60}-substituted derivative. To gauge the influence of this effect, we have repeated the same transfer-rate calculations for hypothetical OPV_n–C_{60} complexes in which C_{60} replaces MPC_{60} and lies next to OPV_n (the donor and acceptor being then no longer chemically bound). The results are shown in Table 1. As expected, within the Förster model, the higher symmetry of the unsubstituted fullerene molecule translates into much smaller transfer rates (in the ns^{-1} range or smaller), except in OPV_2–C_{60} (because of spectral overlap between emission from the short conjugated segment and absorption into the higher-lying optically allowed T_{1u}-symmetry excited states of C_{60}). In contrast, the multicentric approach applied in the improved Förster model yields very similar excitation hopping times in both series of molecules.

Thus, the electronic couplings promoting energy transfer from OPV_n to MPC_{60} in the dyads investigated here arise mostly from local interactions between the donor and acceptor excited-state wavefunctions, rather than from the finite transition dipoles that follow from lifting the I_h symmetry. As noted by Scholes,[30] this is a typical example where one needs to average over the couplings between the wavefunctions (as done in the multicentric approach adopted here) rather than average over the wavefunctions and then coupling them (as assumed in the point-dipole model or its multipolar extensions). RET to a dipole-forbidden excited state has also been reported by Hsu et al. in the case of carotenoids.[31] From the mere point of view of electronic couplings and energy transfer, the reduced symmetry of C_{60}-substituted derivatives has, thus, a limited impact.

We have applied an atomistic model based on a quantum-chemical description of the electronic excitations to study resonant energy transfer in OPV_n–MPC_{60} dyads. Fast (sub-picosecond) energy transfer is found to take place from the oligophenylene to the C_{60} derivative, as a result of the presence of multiple pathways involving low-lying excited states of the MPC_{60} acceptor. We have shown that it is essential to go beyond the point-dipole approximation assumed in Förster theory to obtain a reliable estimate of the electronic couplings mediating the energy-hopping process. When accounting for all relevant channels in a multicentric transition-density approach, energy-transfer rates in good agreement with experiment are obtained. Our results suggest that charge generation in C_{60}-based dyads might proceed from the fullerene local excited state, i.e., after energy transfer to the electron acceptor.

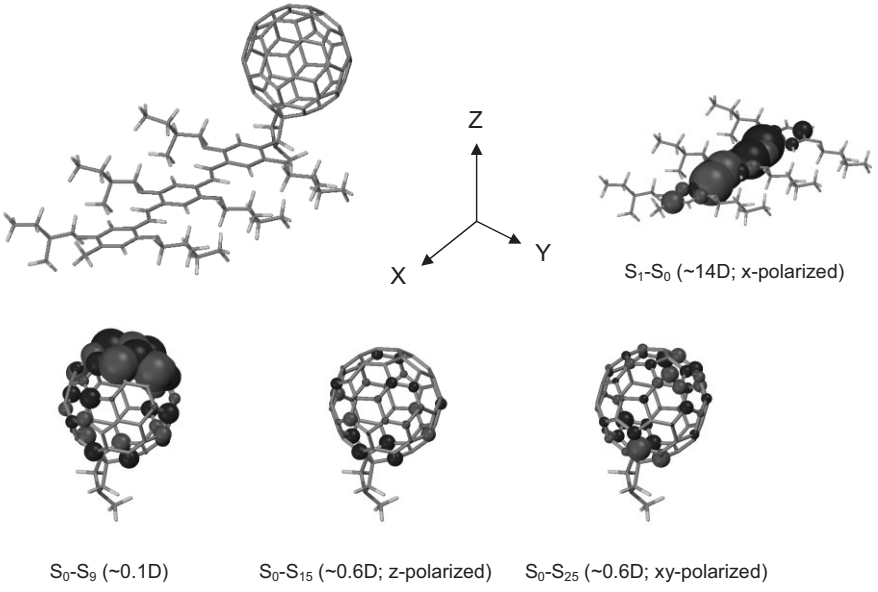

Figure 3. Transition-density distributions calculated at the INDO/SCI level for the electronic excitations in MPC_{60} that contribute the most to the energy-transfer rates in OPV_n–MPC_{60} dyads; the transition densities to the lowest excited state in OPV_3 are shown for comparison. The geometric structure of OPV_3–MPC_{60} is shown on top together with the *xyz* reference frame.

Although care should be taken before generalizing these results to other systems, the present work clearly emphasizes the need to consider both energy-transfer and electron-transfer processes in order to obtain a complete picture of the photophysics at organic–organic heterojunctions. For the operation of polymer solar cells, the utilization of RET provides an interesting option to direct exciton migration to the interface of donor and acceptor more rapidly and over longer distances than random hopping of excitons.[13] Surprisingly, the role of RET in exciton transport in bulk heterojunctions has not received much attention, although it is likely to be operative in any combination of materials with different optical gaps and can play a crucial role as far as harvesting sunlight is concerned. Presently, one of the main limiting factors to the charge-generation external quantum yields achieved in polymer–fullerene-based solar cells is the rather poor match between solar emission and absorption from the photoactive components of the cell. It is therefore not a surprise that the design of low-bandgap conjugated polymers has attracted much attention recently.[32,33] It would be interesting to develop material combinations incorporating low-bandgap polymers that give rise to an even lower energy state at the interface of two components. Such interface states could efficiently collect excitons via directional transport from both components.

Experimental

The chemical structures of the investigated OPV_n–MPC_{60} ($n = 2$–4) molecules are shown in Figure 4. The ground-state geometries of the dyads were first optimized at the semiempirical AM1 level [34]. Next, the AM1 method was coupled to a complete active space configuration interaction (CAS-CI) scheme to compute the excited-state geometries of the isolated OPV_n oligomers [35]. In the weak-coupling regime, RET indeed occurs from the thermalized donor excited state, i.e., after full geometric relaxation over the donor. The structure of the complete dyad systems was finally built by inserting the OPV_n* excited-state geometry in the OPV_n–MPC_{60} ground-state structure.

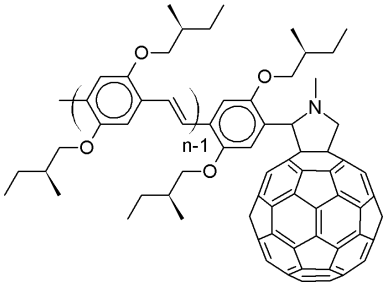

Figure 4. The molecular structure of OPV_n–MPC_{60}, $n = 2$–4.

The INDO Hamiltonian [36] was combined to a single-configuration-interaction (SCI) scheme to describe the electronic excitations in the OPV_n and MPC_{60} isolated fragments [37]. On the basis of the excited-state properties provided by the INDO/SCI scheme, the total rate for RET from the OPV to the fullerene derivative was calculated by summing the hopping rates over all acceptor states:

$$k_{\mathrm{RET}} = \sum_{j_a} k_{i_d - j_a} \tag{1}$$

where i_d denotes the lowest donor (OPV_n) excited state (involved in donor emission) and j_a runs over all acceptor (MPC_{60}) excited states located within 5 eV of the ground state (such a large spectral range grasps all acceptor states with significant spectral overlap with donor emission and ensures full convergence of the results). Each term in the summation corresponds to a pathway for energy migration and contributes a partial rate given by Equation 2 (the Fermi golden rule) in the weak-coupling approximation [38]:

$$k_{i_d - j_a} = \frac{2\pi}{\hbar} V^2_{i_d - j_a} J_{i_d - j_a} \tag{2}$$

where $\hbar = h/2\pi$ (h is Planck's constant). The electronic couplings for the different channels in Equation 2 are readily obtained from the corresponding atomic-transition densities as computed at the INDO/SCI level on the basis of the AM1-AM1/CAS-CI geometries:

$$V_{i_d - j_a} = \frac{1}{4\pi\varepsilon_0} \sum_m \sum_n q_{i_d}(m)\, q_{j_a}(n)\; V(m,n) \tag{3}$$

where m and n run over all atomic sites on the donor i_d and the acceptor j_a excited states; $q_{i_d}(m)$ ($q_{j_a}(n)$) denotes the atomic transition density on site m (n) for the donor (acceptor) state i_d (j_a); $V(m,n)$ is the Coulomb potential in atomic representation, which is taken here as the Mataga–Nishimoto [39] potential.

A displaced harmonic-oscillator model was applied to numerically compute the normalized absorption and emission spectra and the spectral-overlap factors in Equation 2 [40,41]. For the OPV_n segment, a simple one-mode vibronic approach was applied with standard parameters that yield photoluminescence spectral shapes in close agreement to experiment: the Huang–Rhys factor was set to 1.0, and the effective vibrational frequency to 0.17 eV. The measured optical-absorption spectra of fullerene derivatives do not show any fine structure, which might be related to their 3D molecular architecture and/or the overlap between many closely lying weak bands, leading to rather broad and featureless spectra [8,9]. Vertical transition energies were thus used in the simulation of the acceptor absorption with no attempt to account for the coupling to vibrations. Both emission and absorption spectra were convoluted using Gaussian functions with 0.1 eV standard deviation (changes in the rates by less than 10 % are obtained when tuning this value from 0.01 to 0.5 eV).

Received: January 24, 2006
Final version: March 14, 2006
Published online: April 12, 2006

[1] R. H. Friend, R. W. Gymer, A. B. Holmes, J. H. Burroughes, R. N. Marks, C. Taliani, D. D. C. Bradley, D. A. dos Santos, J.-L. Brédas, M. Lögdlund, W. R. Salaneck, *Nature* **1999**, *397*, 121.

[2] J.-L. Brédas, J. Cornil, D. Beljonne, D. A. dos Santos, Z. Shuai, *Acc. Chem. Res.* **1999**, *32*, 267.

[3] *Primary Photoexcitations in Conjugated Polymers: Molecular Exciton versus Semiconductor Band Model* (Ed: N. S. Sariciftci), World Scientific, Singapore **1997**.

[4] R. Kersting, U. Lemmer, M. Deussen, H. J. Bakker, R. F. Mahrt, H. Kurz, V. I. Arkhipov, H. Bässler, E. O. Göbel, *Phys. Rev. Lett.* **1994**, *73*, 1440.

[5] S. E. Shaheen, C. J. Brabec, N. S. Sariciftci, F. Padinger, T. Fromherz, J. C. Hummelen, *Appl. Phys. Lett.* **2001**, *78*, 841.
[6] P. Schilinsky, C. Waldauf, C. J. Brabec, *Appl. Phys. Lett.* **2002**, *81*, 388.
[7] J. C. Hummelen, B. W. Knight, F. LePeq, F. Wudl, *J. Org. Chem.* **1995**, *60*, 532.
[8] E. Peeters, P. A. van Hal, J. Knol, C. J. Brabec, N. S. Sariciftci, J. C. Hummelen, R. A. J. Janssen, *J. Phys. Chem. B* **2000**, *104*, 10 174.
[9] P. A. van Hal, R. A. J. Janssen, G. Lanzani, G. Cerullo, M. Zavelani-Rossi, S. De Silvestri, *Phys. Rev. B* **2001**, *64*, 075 206.
[10] P. A. van Hal, R. A. J. Janssen, G. Lanzani, G. Cerullo, M. Zavelani-Rossi, S. De Silvestri, *Chem. Phys. Lett.* **2001**, *345*, 33.
[11] C. J. Brabec, G. Zerza, G. Cerullo, S. De Silvestri, S. Luzzati, J. C. Hummelen, N. S. Sariciftci, *Chem. Phys. Lett.* **2001**, *340*, 232.
[12] P. A. van Hal, S. C. J. Merkers, R. A. J. Janssen, *Appl. Phys. A* **2004**, *79*, 41.
[13] D. Gonzalez-Rodriguez, T. Torres, D. M. Guldi, J. Rivera, L. Echegoyen, *Org. Lett.* **2002**, *3*, 335.
[14] S. S. Gayathri, A. Patnaik, *Chem. Phys. Lett.* **2005**, *414*, 198.
[15] Y. Liu, M. A. Summers, C. Edder, J. M. J. Fréchet, M. D. McGehee, *Adv. Mater.* **2005**, *17*, 2960.
[16] S. C. J. Meskers, J. Hübner, M. Oestereich, H. Bässler, *J. Phys. Chem. B* **2001**, *105*, 9139.
[17] E. J. W. List, R. Guentner, P. Scanducci de Freitas, U. Scherf, *Adv. Mater.* **2002**, *14*, 374.
[18] L. Chen, D. W. McBranch, H.-L. Wang, R. Helgeson, F. Wudl, D. G. Whitten, *Proc. Natl. Acad. Sci. USA* **1999**, *96*, 12 287.
[19] P. E. Keivanidis, J. Jacob, L. Oldridge, P. Sonar, B. Carbonnier, S. Baluschev, A. C. Grimsdale, K. Müllen, G. Wegner, *ChemPhysChem* **2005**, *6*, 1650.
[20] J.-L. Brédas, D. Beljonne, V. Coropceanu, J. Cornil, *Chem. Rev.* **2004**, *104*, 4971.
[21] See, e.g., G. D. Scholes, *Annu. Rev. Phys. Chem.* **2003**, *54*, 57.
[22] S. Marguet, D. Markovitsi, P. Millie, H. Sigal, S. Kumar, *J. Phys. Chem. B* **1998**, *102*, 4697.
[23] D. Beljonne, J. Cornil, R. Silbey, P. Millié, J.-L. Brédas, *J. Chem. Phys.* **2000**, *112*, 4749.
[24] G. D. Scholes, I. R. Gould, R. J. Cogdell, G. R. Fleming, *J. Phys. Chem. B* **1999**, *103*, 2453.
[25] H. Wiesenhofer, D. Beljonne, G. D. Scholes, E. Hennebicq, J.-L. Brédas, E. Zojer, *Adv. Funct. Mater.* **2005**, *15*, 155.
[26] K. F. Wong, B. Bagchi, P. J. Rossky, *J. Phys. Chem. A* **2004**, *108*, 5752.
[27] a) T. Förster, *Ann. Phys.* **1948**, *2*, 55. b) T. Förster, *Discuss. Faraday Soc.* **1959**, *27*, 7. c) T. Förster, *Pure Appl. Chem.* **1970**, *42*, 443.
[28] G. Orlandi, F. Negri, *Photochem. Photobiol. Sci.* **2002**, *1*, 289.
[29] S. Leach, M. Verloet, A. Desprès, E. Breheret, J. P. Hare, T. J. Dennis, H. W. Kroto, R. Taylor, D. R. M. Walton, *Chem. Phys.* **1992**, *160*, 451.
[30] G. D. Scholes, *Annu. Rev. Phys. Chem.* **2003**, *54*, 57.
[31] C. P. Hsu, P. J. Walla, M. Head-Gordon, G. R. Fleming, *J. Phys. Chem. B* **2001**, *105*, 11 016.
[32] A. Dhanabalan, J. K. J. van Duren, P. A. van Hal, J. L. J. van Dongen, R. A. J. Janssen, *Adv. Funct. Mater.* **2001**, *11*, 255.
[33] X. Wang, E. Perzon, J. L. Delgado, P. de la Cruz, F. Zhang, F. Langa, M. Andersson, O. Inganäs, *Appl. Phys. Lett.* **2004**, *85*, 5081.
[34] a) M. J. S. Dewar, E. G. Zoebisch, E. F. Healy, J. J. P. Stewart, *J. Am. Chem. Soc.* **1985**, *107*, 3902. b) AMPAC 8, 1992–2004 Semichem, Inc. PO Box 1649, Shawnee, KS 66 222.
[35] The CI active space was chosen to ensure converged geometric parameters and includes the most frontier molecular orbitals (typically ten molecular orbitals).
[36] J. Ridley, M. C. Zerner, *Theor. Chim. Acta* **1973**, *32*, 111.
[37] For MPC_{60}, the CI active space includes all possible excitations from the 70 highest to the 70 lowest molecular orbitals; all π-orbitals are included for the OPV_n donors.
[38] E. Hennebicq, G. Pourtois, G. Scholes, L. M. Herz, D. M. Russell, C. Silva, S. Setayesh, A. C. Grimsdale, K. Müllen, J.-L. Brédas, D. Beljonne, *J. Am. Chem. Soc.* **2005**, *127*, 4744.
[39] N. Mataga, K. Z. Nishimoto, *Phys. Chem.* **1957**, *13*, 140.
[40] M. Lax, *J. Chem. Phys.* **1952**, *20*, 1752.
[41] *Charge and Energy Transfer Dynamics in Molecular Systems* (Eds: V. May, O. Kühn), Wiley-VCH, Berlin **2003**.